Journal of the European Ceramic Society 21 (2001) 727–735

www.elsevier.com/locate/jeurceramsoc

Fabrication of tubular electrolytes for solid oxide fuel cells using strontium- and magnesium-doped $LaGaO_3$ materials

Yanhai Du *, N.M. Sammes [1]

Department of Materials and Process Engineering, The University of Waikato, Private Bag 3105, Hamilton, New Zealand

Received 20 June 2000; received in revised form 16 August 2000; accepted 22 August 2000

Abstract

Long, straight, dense, and even-shaped tubular electrolytes (200–300 mm in length, 2.4–2.5 mm inside diameter and 0.3–0.4 mm wall thickness) were successfully fabricated from strontium- and magnesium-doped $LaGaO_3$ materials by way of extrusion. An economic and practical process was developed to extrude the small tubes using water-based and organic-based additives and optimized process parameters. Particle size distribution and specific surface area of the synthesized powder were modified by calcination and ball milling. Obtaining workable pastes played an important role in achieving smooth, linear, even and dense green tubes. The final products showed a dense microstructure and improved mechanical strength over pressing routes. Modulus of rupture of the extruded materials was found to be 180±16 MPa at room temperature and 113±11 MPa at 800°C.

Keywords: Extrusion; Fuel cells; $LaGaO_3$; Mechanical properties; Microstructure-final

1. Introduction

With its high energy conversion efficiency and fuel flexibility, the solid oxide fuel cell (SOFC) has been attracting increasing attention recently. The design and fabrication of SOFCs are critical issues for its development and commercialization. To date, the SOFC has three main designs under scrutiny, namely the tubular, planar, and monolithic designs. The tubular SOFC is based upon a single cell of tubular geometry, which has good thermal performance.

Yttria-stabilized zirconia (YSZ) is a typical electrolyte material for use in SOFCs. However, YSZ requires a high operation temperature (800–1000°C) environment to provide sufficient oxygen ion conductivity. The cost of manufacturing these devices is proving to be unsatisfactorily high, primarily because expensive high temperature alloys must be used for the balance-of-plant structures. These costs would be substantially reduced if the operating temperature could be lowered to between 600 and 800°C, allowing the use of cheaper structural components, such as stainless steel. To lower the operating temperature of SOFCs, either the conductivity of YSZ must be improved by using, for example, thin film technology, or alternative electrolyte materials must be developed to replace YSZ. A concerted effort is being made by researchers to develop such materials. Ceramics that are currently being investigated include Gd-doped CeO_2[1–3] and (Sr, Mg)-doped $LaGaO_3$ (LSGM).[4–6]

Strontium- and magnesium-doped lanthanum gallate, as a high oxide-ion conductor for use in intermediate temperature SOFCs was first reported by Ishihara et al.,[7] and was shown to exhibit a high ionic conductivity over a wide range of oxygen partial pressure. The electrical properties and crystal structure were investigated in great detail recently by Huang et al.,[8] while the mechanical and physical properties of $La_{0.8}Sr_{0.2}Ga_{1-x}Mg_xO_{3-\delta}$ ($x=0.02$–0.20) were examined by Sammes et al.[9,10] and Baskaran et al.[11] For $La_{0.8}Sr_{0.2}Ga_{0.8}Mg_{0.2}O_{3-\delta}$, the modulus of rupture of bars was found to be 113±8 MPa at room temperature,[9] and 90 MPa at 800°C.[10]

This paper focuses on the fabrication of tubular electrolytes for SOFC, using LSGM materials, and describes the fabrication procedure, parameter determination, and the additive selection. The mechanical strength and

* Corresponding author at current address: Acumentrics Corporation, 14 Southwest Park, Westwood, MA 02090-1548, USA. Fax: +1-781-4611759.

E-mail address: ydu@acumentrics.com (Y. Du).

[1] Current address: Acumentrics Corporation, 14 Southwest Park, Westwood, MA 02090-1548, USA.

0955-2219/01/$ - see front matter
PII: S0955-2219(00)00257-0

the microstructure of the sintered products were also examined and are presented in order to better understand the extruded materials and compare with the previous studies, in which the samples were formed by non-extrusion methods.

2. Materials and experimental procedure

Raw materials used to synthesize LSGM were: La_2O_3 (99.9%), Ga_2O_3 (99.99%), and MgO (99+%) (all from Aldrich Chemical Company Inc.), $SrCO_3$ (99+%) (AJAX Chemicals). Binders and other additives used for extrusion in this work were B1501 and B1502 (Dramax™, Rhom and Haas Formulation Chemicals), PEG-400 (Union Carbide Co.), and AMP-95 (Angus Chemical); Hypermer PS-3 (Uniqema), PVB (Polyvinyl butyral, Aldrich Chemicals Inc.), and Octanol-1 (BDH).

Two LSGM powders, which were synthesized using a solid state method and a coprecipitation technique, were used in this study. For the solid state method, stoichiometric quantities of the lanthanum oxide (pre-calcined at 1500°C), magnesium oxide (pre-calcined at 1000°C), gallium oxide, and strontium carbonate were thoroughly mixed and then isostatically pressed into discs at 200 MPa, following by firing at 1500°C for 12 h. The sintered discs were ground using an alumina mortar and pestle, and then milled in a 250 ml Neglene container with acetone and 10 mm diameter zirconia grinding media. This wet ball milling process was found more efficient than dry ball milling which caused agglomeration and produced fewer submicron particles. Coprecipitated LSGM powder was provided by Anan Kasei Co. Ltd, Japan. The as-received coprecipitated powder was calcined at 800–1400°C and then milled for up to 72 h in order to modify the surface area and particle size. The effects of the calcination temperature and milling time on the particle size and specific surface area were studied.

The procedures used to extrude LSGM tubes were similar to our previous work on YSZ tubes.[12] The binders, surfactants, and plasticizers were added into the desirable powders, mixed and milled in solvents to create slurries. The slurries were dried in air by pouring them onto plastic or glass sheets. The mixture was removed from the sheets after most of the solvent had evaporated from the slurries. Pastes were produced through aging the mixture in plastic bags. Workable pastes were extruded into tubes or rods using a piston extruder, as shown in Fig. 1. A load was placed on the top of the piston causing it to move down at a speed of 3 mm/min, which in turn forced the paste to go through the die to form a tubular geometry. The loads needed for extrusion of the tubes varied from between 5 and 10 kN depending on the flexibility of the dough. Efforts were made to keep the green tubes straight and to ensure that the tubular geometry shape was kept during the drying and handling processes. The green extrudates were completely dried in air and then in an oven before sintering. The sintering regime was determined according to the results realized from the differential thermal analysis (DTA, TA Instruments) measurement. The effects of sintering temperature (1450–1520°C) and dwelling time (2–72 h) on the microstructure of the sintered products were examined.

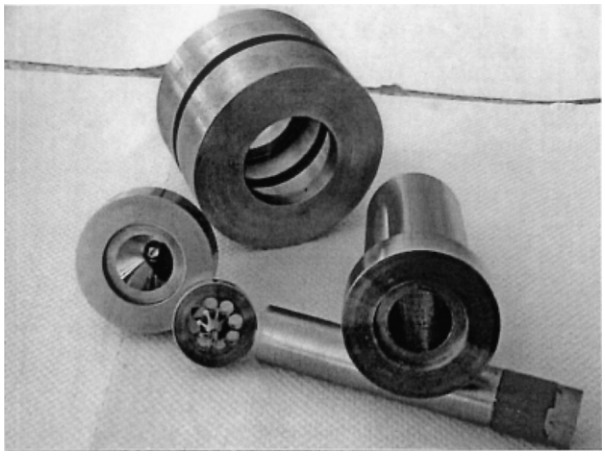

Fig. 1. Photograph of the extrusion device.

Extrusion was carried out on a standard LLOYD LR100 K tensile testing machine coupled to a personal computer. A scanning electron microscope (SEM, Hitachi S4000) and an X-ray diffractometer (Philips X'pert-MPD PW3035) were employed to inspect the microstructure and crystal structure of the products. Particle size analysis was performed using a laser diffraction particle sizer (Malvern Masterizer). Surface area of the powder was determined using the BET (Brunauer–Emmett–Teller) method, and the measurement was carried out on a standard gas sorption analyzer (NOVA-1000, Quantachrome Co.). After degassing overnight at 150°C, powder samples were analyzed and three-point BET data were collected. A particle charge detector (Mütek PCD 03) was used to measure the particle surface charge. Modulus of rupture (MOR) of the materials was tested on an Instron instrument at room temperature and 800°C in air. The lower span was 8.34 mm and the crosshead speed was 0.2 mm/min. Flexure samples of 12 mm in length were either extruded and sintered rods (2 mm in diameter) or bars (2×2 mm). Bar shape samples were cut from sintered discs and the surfaces were ground and polished to 1 μm finish.

3. Results and discussion

3.1. Powder synthesis

Room temperature and high temperature (900°C) powder X-ray diffraction patterns, as shown in Fig. 2,

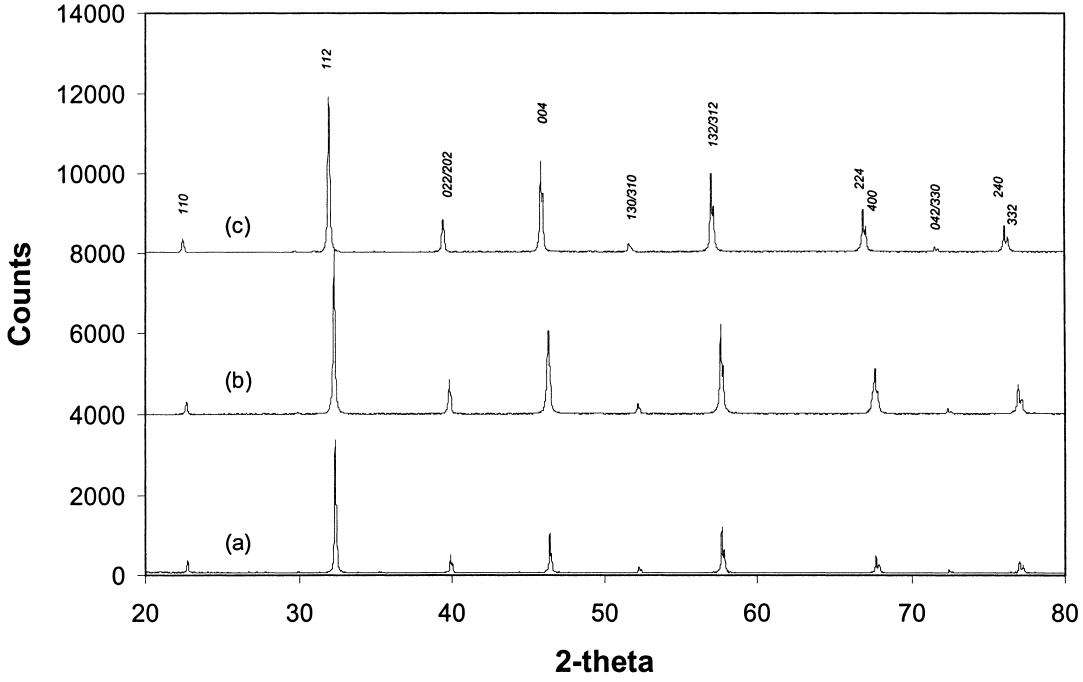

Fig. 2. Room temperature and high temperature powder X-ray diffraction patterns of the material synthesized by solid state technique and coprecipitation method: (a) coprecipitated powder, room temperature; (b) solid state powder, room temperature; (c) solid state powder, 900°C.

indicated that the material synthesized from both solid state and coprecipitation techniques was single perovskite phase, which remained unchanged up to 900°C. Particle morphology is one of the most important factors affecting the microstructure of green components. The powder prepared from the coprecipitation technique consisted of loose and porous agglomerates with rough surfaces, which had very high specific surface area (7.6 m^2/g) and required a large amount of solvents and binders for extrusion. Consequently, pre-treatment of the coprecipitated powder became necessary.

3.2. Particle size and surface area study

Particle size plays an important role in ceramic extrusion processes to achieve a dense material. SEM and BET results (Figs. 3 and 4) showed that calcination was an efficient way to reduce the particle surface area and thus achieve a dense sintered product. Powders calcined at 1000 and 1200°C showed porous structures, and those fired at 1400°C showed densification. Compared with the uncalcined powder (Fig. 3a) and the powders calcined at lower temperatures (Fig. 3b,c), the powders fired at 1400°C (Fig. 3d) required lower amounts of additives for extrusion to occur because of the reduced specific surface area (from 7.6 to 0.3 m^2/g, see Fig. 4). However, the maximum particle size of the calcined powder (Fig. 5) was too large to be used in extruding very small tubes. The wall thickness of the sintered tubes in this project is only 0.3–0.4 mm. With such large particles it is also very hard to get a smooth surface finished tube. And, moreover, in order to achieve effective and dense particle packing, the powder must have a certain particle size distribution. Thus, the fired powders were milled for up to 72 h. After milling, we obtained a wide range of particle size distribution, which could be divided into three groups <1, $1\sim10$ and >10 μm (fine, medium, and coarse). The amount of small and large particles over different milling times is as described in Fig. 6. The number of large particles (>10 μm) decreased significantly after ball milling. We examined the surface area again after milling, and the specific surface area had consequently increased, as shown in Fig. 7. From the powder property study we recognized that a balance between the particle size and the surface area should be made in order to obtain a desirable extrudate.

3.3. Selection of binders and preparation of extrudable pastes

In order to make the ceramic powder extrudable, additives are required. These additives normally include binders, lubricant, plasticizer, dispersant, and solvent. Binders provide strength to the green tubes after evaporation of the solvent. Surfactants reduce the interfacial tension between the surface of the particle and the liquid to improve wetting and dispersion. Plasticizers increase the flexibility and workability of the paste by modifying the viscoelastic properties of a condensed binder-phase film on the particles, but they tend to reduce the green product strength. Solvents dissolve the

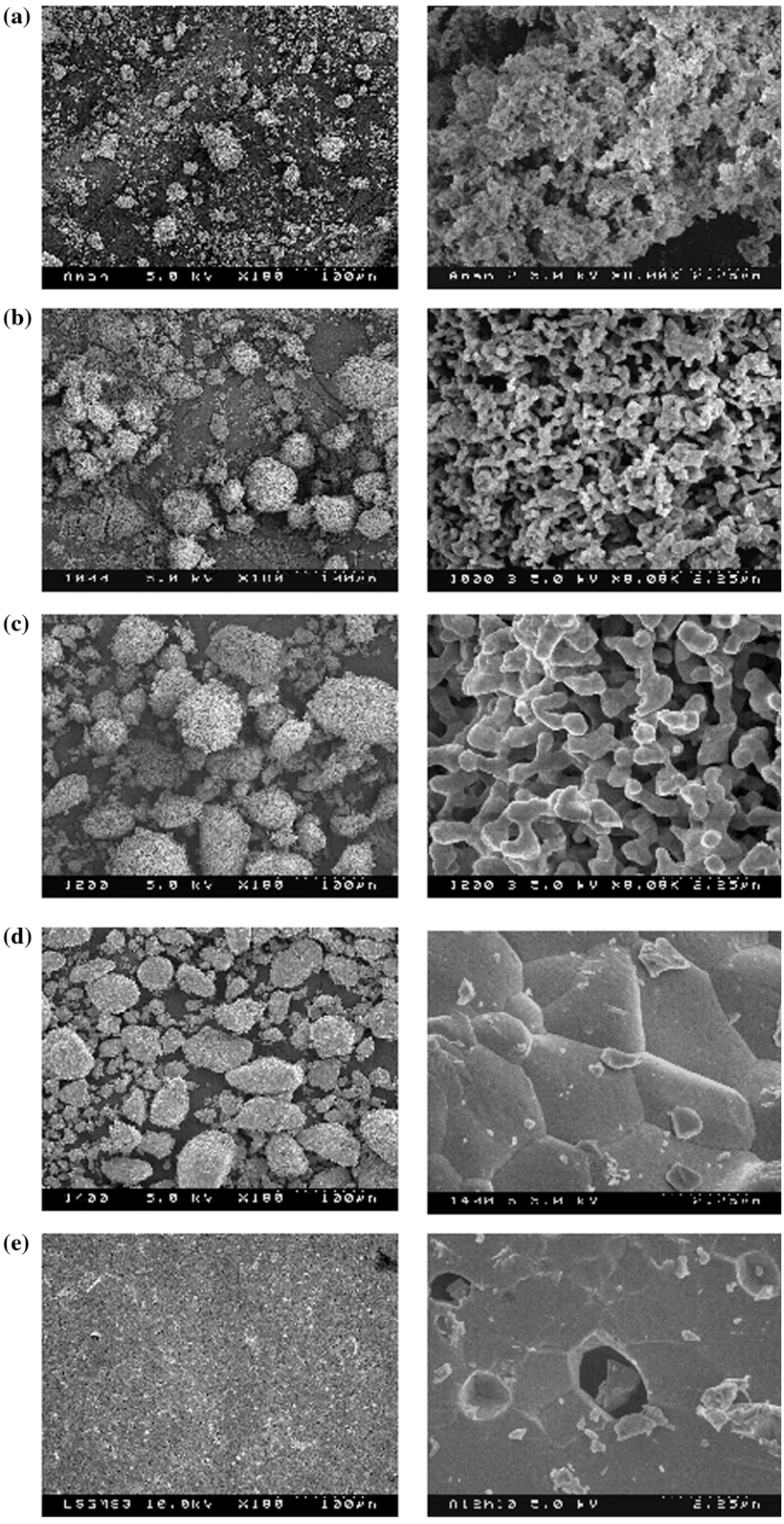

Fig. 3. Micrographs of the as-received coprecipitated powder and after calcination for 2 h at different temperatures: (a) as-received, (b) 1000°C, (c) 1200°C, (d) 1400°C, (e) fracture cross section of a pallet calcined at 1400°C.

organic materials and distribute them uniformly throughout the slurry. Two systems of additives, namely organic based systems and water-based systems, were studied. PVB (Polyvinyl butyral) is one of the most popular organic binders, which can be dissolved in acetone but not in water due to its non-polar and non-ionic nature. Together with surfactant PS-3 and plasticizer octanol-1, this system worked well with the LSGM powders. The amount of octanol-1 influenced the workability of the pastes and the extrudates. Too much of the plasticizer led to tacky products, which did not remain straight on handling; conversely, too little caused cracks while drying and sintering. B1051 and B1052 are specific binders for ceramic extrusion, which are soluble in both acetone and water. B1051/B1052 system, plus plasticizer PEG-400 and surfactant/pH control agent AMP-95, was suitable for powder synthesized from the solid state technique. However, coagulation and flocculation occurred when adding them into the solutions synthesized from the coprecipitated powder. This was postulated as being due to the big differences in surface charges of the two powders. Surface charge of the powders prepared by coprecipitation and solid state techniques were $(1.5–2)\times10^{-6}$ eg/g and 0.08×10^{-6} eg/g, respectively, measured using a particle charge detector described in part II. The coprecipitated

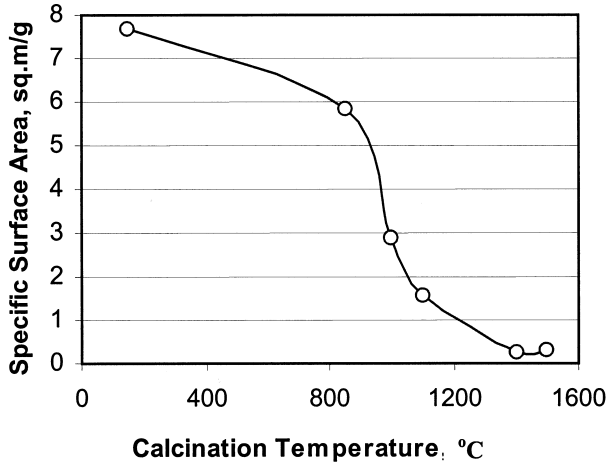

Fig. 4. Specific surface area of the powders after calcination at different temperatures.

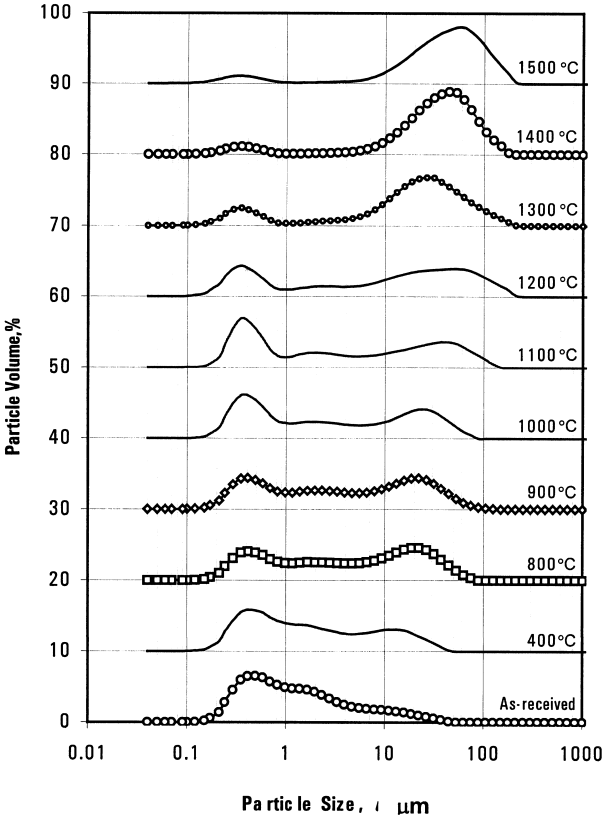

Fig. 5. Particle size distribution of the powders calcined for 2 h at different temperatures.

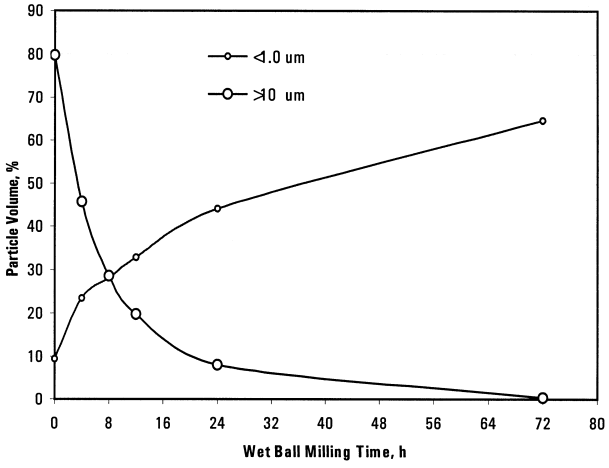

Fig. 6. Particle size contribution of the calcined powder after wet ball milling for different times.

powder, with a high positive surface charge, easily

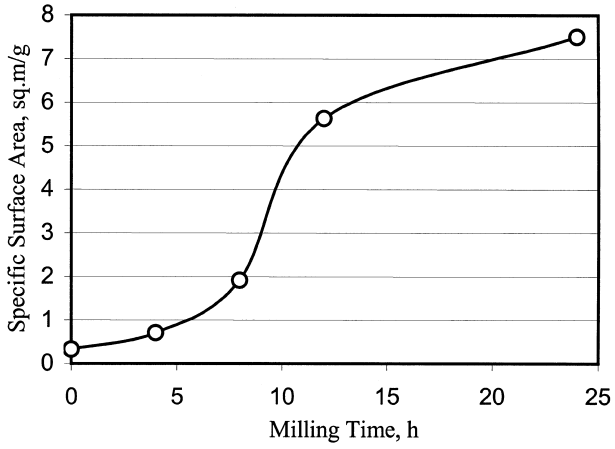

Fig. 7. Specific surface area of the calcined powder after wet ball milling for different times.

attracts uncharged or negatively charged particles to form coagulations. The exact mechanism that caused the coagulation is however unclear.

Table 1 lists the formulation of the additives tested in this work. The amount of solvents and plasticizers was altered to adjust the flowability of the slurries and the workability of the pastes according to the characteristics and the specific surface area of the powders. Powder was first mixed and ground with the surfactants in the solvent by means of a roller mill for 4–12 h. Binders and plasticizers were then added and milled for a further 1–2 h. Addition of solvent was sometimes required to keep the slurry running after adding the binders, and to adjust the slurry layer thickness for the drying process. The solvent content variation at every stage is demonstrated in Fig. 8. Desirable slurries contained 100–120% of solvents, while workable pastes contained 3–5% of solvents when extruding.

Table 1
Formulations of the additives tested for extruding LSGM tubes

	Binders	Solvent	Surfactant	Plasticizer
Water-based system	B1051 B1052 8.3% 4.6%	Acetone Water 110–170% 0–20%	AMP-95 0–1.8%	PEG-400 6.6%
Organic-based system	PVB 6–8%	Acetone 100–120%	PS-3 2–5%	Octanol-1 1.5–6%

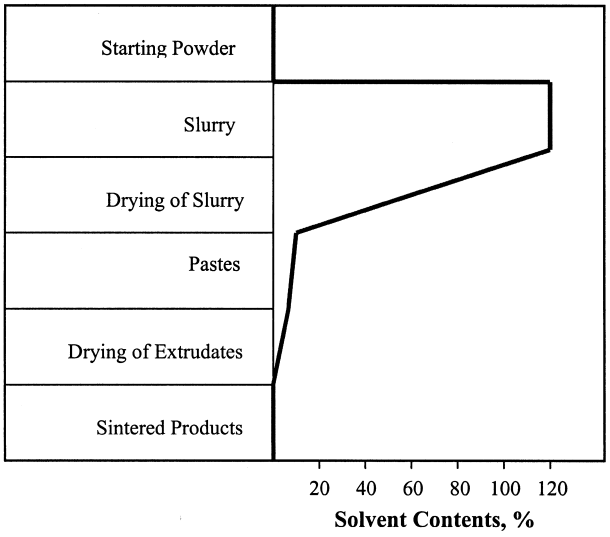

Fig. 8. Solvent content variation during the processing.

3.4. Extrusion

A tubular geometry shape was formed by extruding the flexible pastes in a piston extruder shown in Fig. 1. The extrusion speed was kept constant at 3 mm/min. The loads required for the extrusion were uncontrollable and depended on the flexibility of the pastes, extrusion speed, and the design of the extrusion apparatus. An extrusion pressure of 15–30 MPa was calculated according to the extrusion load recorded in this work. The micrograph of the green tube (Fig. 9) revealed that the voids may formed at the extrusion stage in the products without deaeration and under low compaction pressure. Some of the pores remained in the sintered products. Glass tubes with suitable diameters were used to catch the green tubes while extruding. The extra benefit of using glass tubes is discussed in Section 5. With this method, 200–300 mm-long green tubes, as shown in Fig. 10, were realized under the extrusion conditions.

3.5. Drying and sintering

Drying is undertaken to remove the liquid from the green products. The control of temperature and moisture for the drying process was undertaken to avoid cracking during and after the evaporation of the solvent from the green body, because of stresses produced by differential

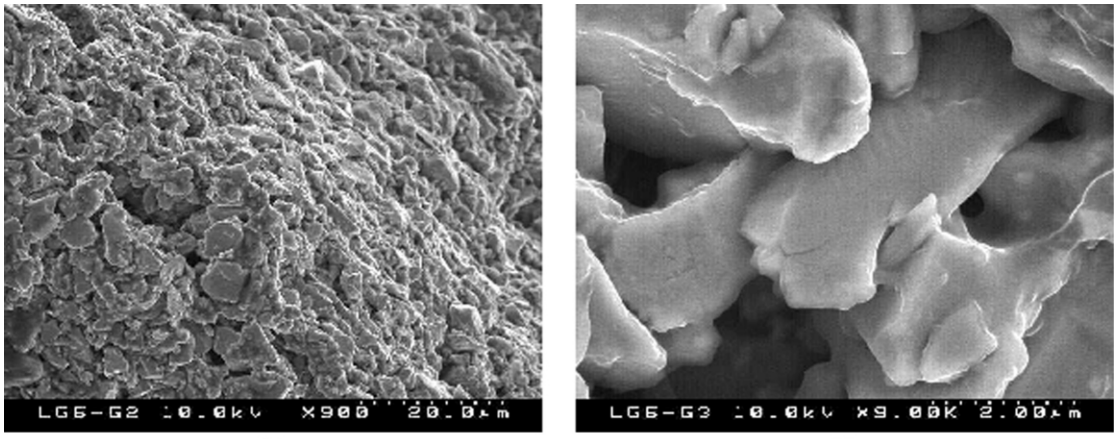

(a) (b)

Fig. 9. Micrographs of the extruded surface (a) and the internal fracture surface (b) of the green LSGM tubes.

shrinkage. To keep the green tubes straight and control the moisture content, they were stored in sealed glass holders immediately after extruding. The glass holders, with the extruded tubes inside, could be slowly rolled by hand or on a roller to maintain the tubular geometry and avoid adhesion. Tubes, fabricated from suitable pastes, were dried at room temperature overnight, and then at 40–100°C in an oven for 4–12 h. The dried body with no cracks detected was then sintered in air.

Solid-state sintering was carried out in order to densify the extruded LSGM products. A slow ramp of 1°C/min from room temperature to 500°C was undertaken to allow the additives to burn-out. A rapid heating rate of 6°C/min above 500°C was used to quickly build up the particle bonding after binder burnout. The effect of sintering temperature (1450–1520°C in air) and dwelling time (2–72 h) were examined and the results are presented in Section 7. In general, dense sintered bodies could be obtained at higher sintering temperatures and/or longer dwelling times. Linear shrinkage of the tubes, during the drying and sintering processes, were calculated and are illustrated in Fig. 11. The sintering shrinkage was approximately 20%.

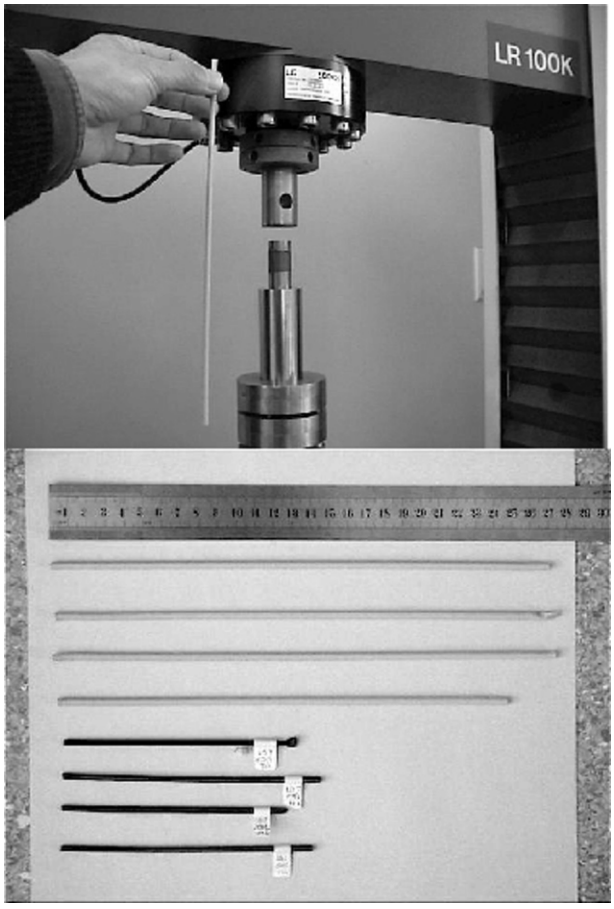

Fig. 10. Photograph of the green (long and light colour) and sintered (short and dark colour) LSGM tubular electrolytes.

Table 2
Comparison of modulus of rupture of the LSGM materials prepared by extrusion and isostatic pressing

Sample prepared by	Test temperature	MOR (MPa)
Isostatic press	RT	147±20
		113±8[9]
	800°C	90[10]
Extruded rods	RT	180±16
	800°C	113±11

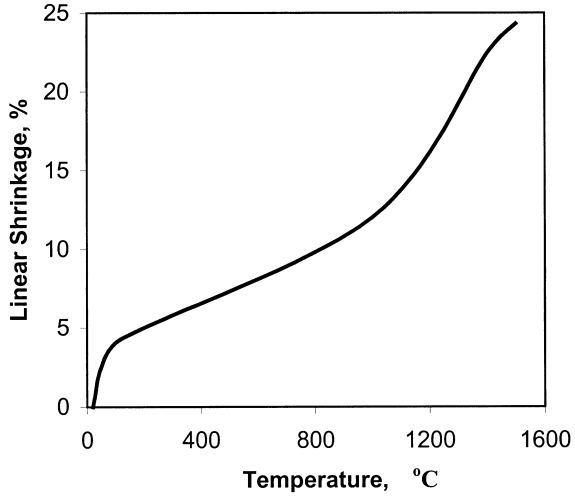

Fig. 11. Linear shrinkage of extruded LSGM tubes during drying and sintering steps.

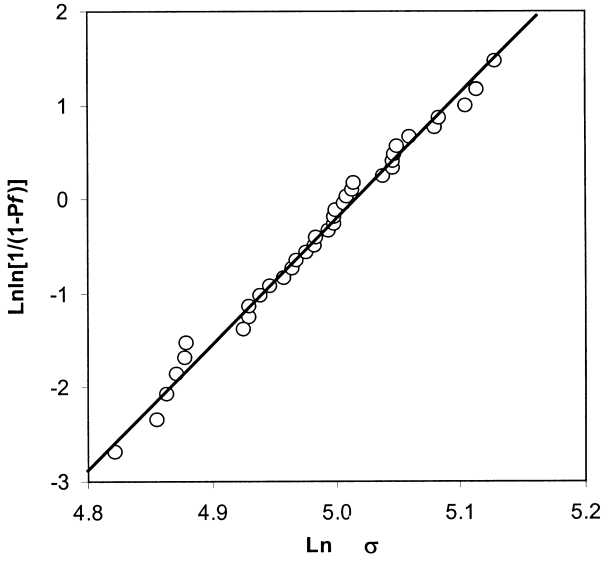

Fig. 12. Weibull plot of the modulus of rupture at room temperature for the extruded LSGM material sintered at 1500°C for 12 h.

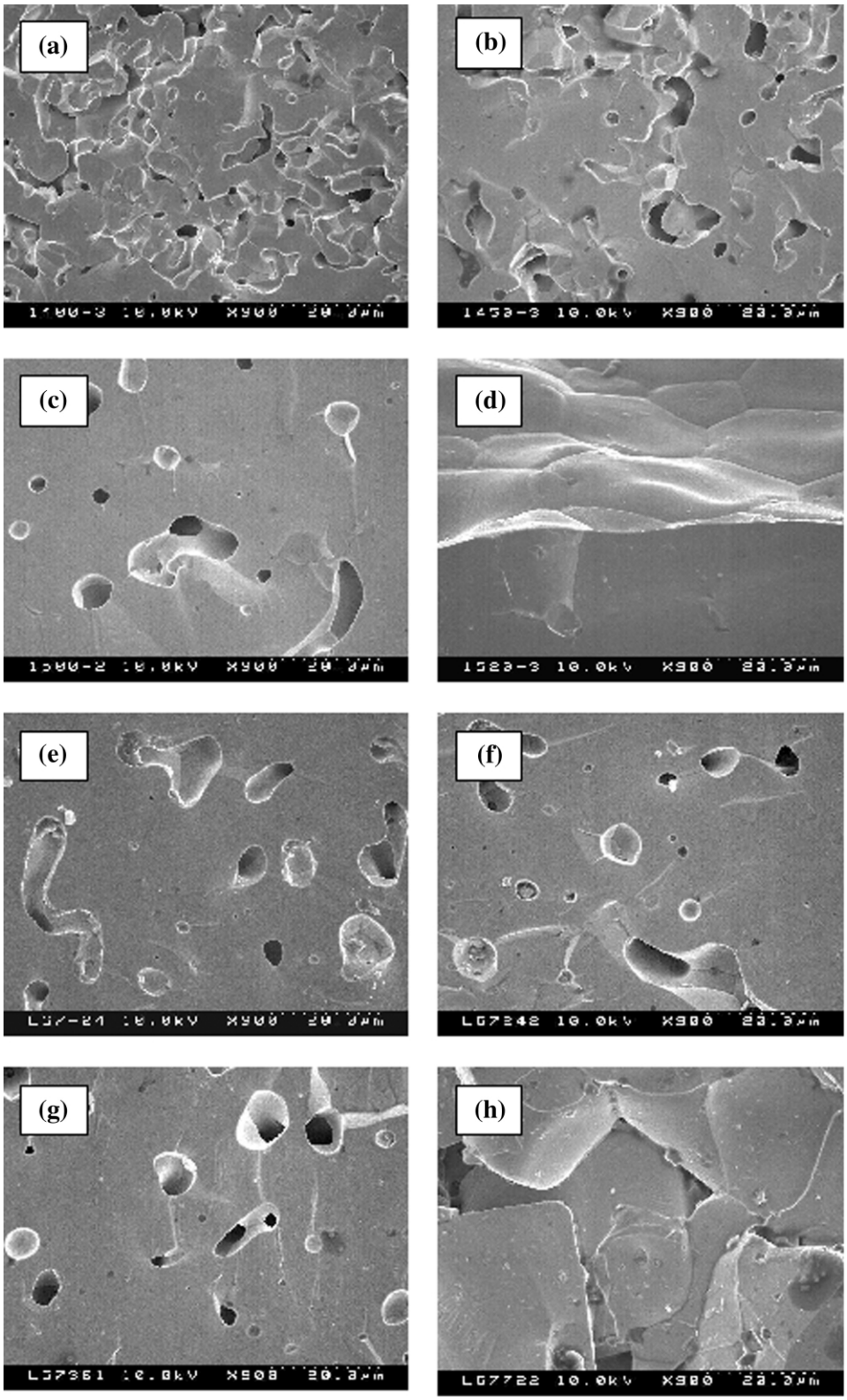

Fig. 13. Effects of the sintering temperature and dwelling time on the SEM microstructures of the extruded LSGM tubular electrolyte: (a) 1400°C for 12 h, (b) 1450°C for 12 h, (c) 1500°C for 12 h, (d) 1520°C for 12 h, (e) 1500°C at 2 h, (f) 1500°C at 24 h, (g) 1500°C at 36 h, (h) 1500°C at 72 h.

3.6. Mechanical properties of the sintered products

Table 2 lists the three-point modulus of rupture (MOR) results of the LSGM materials prepared by extrusion (rods) and use of isostatic press (bars), together with the available reference data for comparison. For isostatic pressed samples the average MOR values were 147±20 MPa. For extruded rods the MOR values were 180±16 MPa at room temperature and 113±11 MPa at 800°C. It is clear that the mechanical strength of the materials is improved by the extrusion fabrication technique. The wet ball milling process and binders are believed to have enhanced the binding strength of the grains after sintering. Further analysis on the mechanical test data, using the Weibull distribution method, indicated that the samples in the three-point bend test (at room temperature) were homogeneous, and the Weibull modulus, m, observed from the slope of the graph (Fig. 12), was 16, which characterized that data spread was in a reliable range.

3.7. Microstructure of the sintered electrolyte

Micrographs of the sintered product (Fig. 13) show that the microstructure of the material approached a dense sintered body with increasing the sintering temperature from 1400 to 1520°C. Irregular or open pores became circular and intersected the grain boundaries. Grain growth caused a reduction in the porosity, which formed during extrusion and after the organic burnout. Prolonging the dwelling duration at 1500°C to over 36 h was not recommended because of the release of gallium from the system, which was confirmed by EDX analysis results. The appearance of the sintered body had changed from a brown color ($\leqslant$36 h) to black (72 h). The strength of the dark material had significantly decreased as the ceramic bonding had been destroyed which produced large pores at the grain boundaries, as can be seen in Fig. 13h. The porosity in the sintered body could be grouped into two distributions by size or shape. The smaller, round micropores with a diameter of 1–3 μm primarily arose from the raw extruding powder (Fig. 3e). Irregular shaped voids were generally formed during the extrusion stage and after the release of the solvents and organic substances from the extrudates.

4. Conclusions

Tubular electrolytes have been successfully extruded using strontium- and magnesium-doped lanthanum gallate ceramic material, and commercially available processing additives. A well-characterized powder is necessary to increase the reliability of the extrusion process. Powder with high density, low specific surface area and a certain particle size distribution, could be obtained by calcination (at 1400°C) and ball milling (for 6–12 h). The microstructure of the final sintered products is largely dependent on the control of the process parameters, especially the workability of the pastes and the sintering temperature of the extrudates. Long, straight, dense and symmetric tubular electrolytes (200–300 mm in length, 2.4–2.5 mm inside diameter and 0.3–0.4 mm wall thickness) could be fabricated by using the procedure developed from this work and the optimized parameters. The modulus of rupture of the material was measured at room temperature (147±20 MPa for isostatic pressed samples, and 180±16 MPa for extruded rods) and high temperature (113±11 MPa at 800°C for extruded rods), which was therefore improved by the extrusion fabrication technique.

References

1. Inaba, H. and Tagawa, H., Review: ceria-based solid electrolytes. *Solid State Ionics*, 1996, **83**, 1–16.
2. Huang, K., Feng, M. and Goodenough, J. B., Synthesis and electrical properties of dense $Ce_{0.9}Gd_{0.1}O_{1.95}$ ceramics. *J. Am. Ceram. Soc.*, 1998, **81**, 357–362.
3. Christie, G. M. and van Berkel, F. P. F., Microstructure — ionic conductivity relationships in ceria-gadolinia electrolytes. *Solid State Ionics*, 1996, **83**, 17–27.
4. Maric, R., Ohara, S., Fukui, T., Yoshida, H., Nishimura, M., Inagaki, T. and Miura, K., Solid oxide fuel cells with doped lanthanum gallate electrolyte and $LaSrCoO_3$ cathode, and Ni-samaria-doped ceria cermet anode. *J. Electrochem. Soc.*, 1999, **146**, 2006–2010.
5. Drennan, J., Zelizko, V., Hay, D., Ciacchi, F. T., Rajendran, S. and Badwal, P. S., Characterisation, conductivity and mechanical properties of the oxygen-ion conductor $La_{0.9}Sr_{0.1}Ga_{0.8}Mg_{0.2}O_{3-x}$. *J. Mater. Chem.*, 1997, **7**, 79–83.
6. Huang, K., Feng, M. and Goodenough, J. B., Sol-gel synthesis of a new oxide-ion conductor Sr- and Mg-doped $LaGaO_3$ perovskite. *J. Am. Chem. Soc.*, 1996, **79**, 1100–1104.
7. Ishihara, T., Matsuda, H. and Talita, Y., Doped $LaGaO_3$ perovskite type oxide as a new oxide ionic conductor. *J. Am. Chem. Soc.*, 1994, **116**, 3081–3083.
8. Huang, K., Tichy, R. S. and Goodenough, J. B., Superior perovskite oxide-ion conductor; strontium- and magnesium-doped $LaGaO_3$: I, phase relationships and electrical properties. *J. Am. Ceram. Soc.*, 1998, **81**, 2565–2575.
9. Sammes, N. M., Keppeler, F. M., Näfe, H. and Aldinger, F., Mechanical properties of solid-state-synthesized strontium- and magnesium-doped lanthanum gallate. *J. Am. Ceram. Soc.*, 1998, **81**, 3104–3108.
10. Sammes, N. M., Keppeler, F. M., Näfe, H., Aldinger, F. and Tompsett, G. A., The high temperature mechanical properties of $La_{0.8}Sr_{0.2}Ga_{0.8-x}Mg_xO_{3-\delta}$. *J. Aust. Ceram. Soc.*, 1998, **34**, 99–105.
11. Baskaran, S., Lweinsohn, C. A., Chou, Y.-S., Qian, M., Stevenson, J. W. and Armstrong, T. R., Mechanical properties of alkaline earth-doped lanthanum gallate. *J. Mater. Sci.*, 1999, **34**, 3913–3922.
12. Du, Y., Sammes, N. M. and Tompsett, G. A., Optimisation parameters for the extrusion of thin YSZ tubes for use as an electrolyte for the SOFC. *J. Eur. Ceram. Soc.*, 2000, **20**(7), 959–965.